RSC Advances

PAPER

View Article Online
View Journal | View Issue

Cite this: *RSC Adv.*, 2024, **14**, 560

Highly selective separation of tetravalent plutonium from complex system with novel phenylpyridine diamide ligands†

Liu Yao, Wang Junli, Le Yuhang, Wang Hui, Wang Wentao, Li Baole and Yan Taihong*

In this study, three phenylpyridine diamide ligands, namely, 2,2′-((pyridine-2,6-diylbis(3,1-phenylene)) bis(oxy))bis(*N*,*N*-diethylacetamide) (PPEA, **L1**), 2,2′-((pyridine-2,6-diylbis(3,1-phenylene))bis(oxy))bis(*N*-ethyl-*N*-phenylacetamide) (PEPA, **L2**), and 2,2′-(((4-phenylpyridine-2,6-diyl)bis(3,1-phenylene))bis(oxy)) bis(*N*,*N*-dioctylacetamide) (PPOA, **L3**), were synthesized and explored for the solvent extraction of Pu(IV) in a HNO_3 medium using 1-(trifluoromethyl)-3-nitrobenzene as the diluent. The effects of HNO_3 concentration, extractant concentration, and temperature on the Pu(IV) extraction efficiency were studied. All three extractants displayed high selectivity for Pu(IV) over other metals such as U(VI), Np(V), Am(III), and various fission elements. At 3 M HNO_3, the distribution ratio for Pu(IV) reached 27.18, in contrast to 1.11, 0.3, and 0.03 for U(VI), Np(V), Am(III), respectively. Slope analysis and UV titration revealed the formation of 1 : 1 $Pu(NO_3)_4$/ligand complexes during extraction. The extraction reactions had negative Gibbs free energies, indicating the spontaneous nature of Pu(IV) extraction at room temperature. Furthermore, the extractants demonstrated good stripping ability and reusability, and their radiolytic stability was reasonable up to an absorbed dose of 100 kGy, underscoring their potential for practical applications. Overall, this study broadens our understanding of actinide–diamide ligand coordination and actinide chemistry during coordination, paving the way for the design and synthesis of new extractants.

Received 31st October 2023
Accepted 5th December 2023

DOI: 10.1039/d3ra07418h

rsc.li/rsc-advances

Introduction

In recent years, the expansion of nuclear energy has led to an increase in spent fuel production, heightening the risks associated with radioactive waste leakage and its detrimental effects on the environment.[1–3] Spent nuclear fuel mainly contains uranium (95%), fission products (4%), and a small amount of plutonium (1%), all of which exhibit significant radioactivity and toxicity.[4–6] The closed nuclear fuel cycle has been identified as an effective strategy to mitigate leakage risks and alleviate environmental concerns.[7–9] Both uranium and plutonium serve as valuable strategic resources. Once recycled, they can be refashioned into nuclear fuel components, with separated plutonium also having potential applications in fast reactors.[7]

Various techniques exist for plutonium separation, including membrane separation,[10,11] adsorption,[12,13] chemical precipitation,[14] ion exchange,[15–18] and solvent extraction.[19–23] Among them, solvent extraction has gained prominence owing to its inherent benefits such as continuous operation, adaptability, radiation stability, and solvent reusability. Several extractants have been utilized, such as tri-*n*-butyl phosphate,[24] trialkyl phosphine oxide,[25,26] octyl-(phenyl) *N*,*N*-diisobutyl carbamoyl methyl phosphine oxide,[27–29] and di-isodecylphosphoric acid.[30] However, the use of phosphorus-containing ligands defies the "CHON" principle, which refers to extractants containing only carbon, hydrogen, oxygen, and nitrogen atoms, and poses serious environmental challenges by generating harmful solid residues. In light of this, researchers have increasingly used amide-based extractants such as *N*,*N*-dihexyl octyl amide,[31] *N*,*N*,*N*′,*N*′-tetraoctyl diglycolamide,[12,32,33] and oxa-bridged bicyclo-dicarboxamide.[34] These extractants not only align with the CHON principle but also offer benefits such as simple synthesis and good chemical irradiation stability. Additionally, the extraction efficiency of amide extractants can be enhanced by modulating the side chains on the nitrogen atoms or the alkyl chains on the amide oxygen atoms.[34–36]

Heterocyclic amide extractants, characterized by their macrocyclic frameworks (Fig. 1), demonstrate superior extraction capabilities for Pu(IV) through multidentate chelation coordination. For example, Zhang *et al.* reported the impressive Pu(IV) extraction capabilities of *N*,*N*′-diethyl-*N*,*N*′-ditolyl-2,9-diamide-1,10-phenanthroline (Et-Tol-DAPhen). However, this extractant also exhibits high distribution ratios for U(VI), Th(IV), and Am(III). Building on this, Shi *et al.* synthesized three new *ortho*-phenanthroline type extractants (Ph-DAPhen, Me-Ph-

Department of Radiochemistry, China Institute of Atomic Energy, P. O. Box 275-26, Beijing 102413, P.R. China. E-mail: yanthcn@163.com

† Electronic supplementary information (ESI) available: Synthesis routes of **L1–L3**, Fig. S1–S4, Tables S1 and S2. See DOI: https://doi.org/10.1039/d3ra07418h

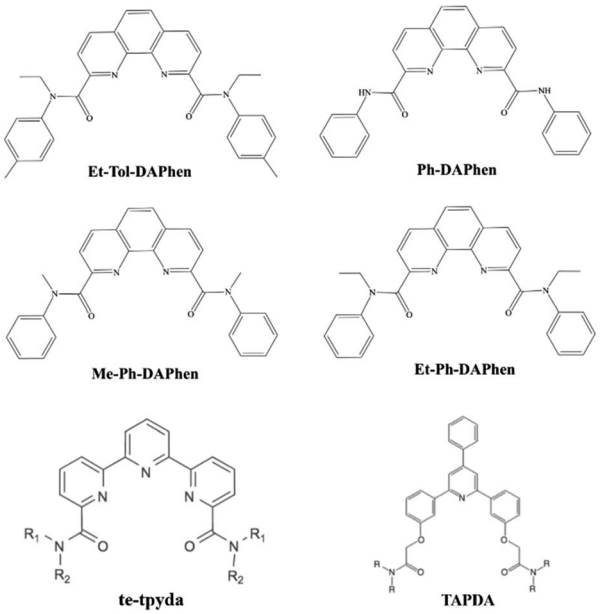

Fig. 1 Structure of heterocyclic amide-based extractants.

DAPhen, and Et-Ph-DAPhen) by adjusting the substituents on the nitrogen atoms. Their investigations revealed that different functional groups, including amide and pyridine groups, influence the extraction performance.[37,38] Additionally, the tripyridine diamide ligand te-tpyda was shown to have good extraction performance for actinide elements. The extractant underwent pentadentate coordination with An(III), and the amide group on its pyridine ring improved its extraction ability for actinide elements by reducing the basicity of the extractant and improving the stability of the metal complex.[39] Sivaramakrishna *et al.* introduced four triarylpyridine diamides (TAPDA) containing three phenyl rings by replacing two pyridine rings connected by an intermediate pyridine ring and then connecting the amide group to the triphenylpyridine group by ether–oxygen bonds.[40] These TAPDA ligands effectively and selectively extracted Pu(IV) at various HNO_3 concentrations. Notably, the distribution ratio of Pu(IV) (D_{Pu}) was 2–4 orders of magnitude higher than those of U, Am, Cm, Cs, and Sr, resulting in promising application potential for the extraction of U/Pu.[40] However, systematic studies on the structure–activity relationships between these extractants and Pu(IV), as well as other actinides, are currently lacking.

In this study, we synthesized three diamide extractants containing phenylpyridine rings: 2,2′-((pyridine-2,6-diylbis(3,1-phenylene))bis(oxy))bis(*N*,*N*-diethylacetamide) (PPEA, **L1**), 2,2′-((pyridine-2,6-diylbis(3,1-phenylene))bis(oxy))bis(*N*-ethyl-*N*-phenylacetamide) (PEPA, **L2**), and 2,2′-(((4-phenylpyridine-2,6-diyl)bis(3,1-phenylene))bis(oxy))bis(*N*,*N*-dioctylacetamide) (PPOA, **L3**) (Fig. 2). We examined the Pu(IV) extraction capabilities of extractants **L1–L3** in HNO_3 using 1-(trifluoromethyl)-3-nitrobenzene as a diluent. We explored the influence of the acidity, extractant concentration, and temperature on the extraction performance, and determined the stable complexation constants and selectivity. We expect this study will enrich the domain of Pu(IV) extraction using diamide ligands and provide a reference for the extraction separation of actinides and the design of new extractants.

Experimental

Chemicals and reagents

All uranium, plutonium, and neptunium radioactive solutions were provided by the China Institute of Atomic Energy (CIAE). Experiments involving radioactivity were conducted in designated facilities adhering to established safety protocols. All reagents were of analytical reagent (AR) grade, and all radioisotopes had a radiochemical purity of above 99.9%.

Experimental equipment

The acidity during the extraction experiments was assessed using an automatic potentiometric titrator (G20S, Mettler Toledo, Switzerland). The mixing and separation of organic and aqueous phases were performed using a multi-tube vortex mixer (LPD2500, Leopard Scientific Instruments, China) and desktop electric centrifuge (TDL80-2B, Shenzhen Anke High-tech Co., Ltd, China), respectively. The radionuclide concentrations of Pu(IV), Am(III), Np(V), and Np(VI) were measured using a liquid scintillator (Tri-Carb 2910 TR, PerkinElmer), while the U(VI) concentrations were determined using an X-ray fluorimeter (LTD, Jing Pu). The concentrations of fission products were determined by inductively coupled plasma (ICP; Thermo Scientific, USA). Ultraviolet-visible (UV-vis) spectrophotometric titration was conducted using a UV spectrometer (Cary 4000, Agilent Technologies, USA). Fourier-transform infrared (FTIR) spectroscopy was performed using an infrared spectrometer (IRAffinity-1S, Shimadzu, Japan).

Solvent extraction experiment

The synthesis routes for ligands **L1–L3** are described in the ESI (Fig. S1),† and the corresponding ^{1}H NMR spectra are displayed in Fig. S2.† The phenylpyridine diamide extractants were dissolved in 1-(trifluoromethyl)-3-nitrobenzene to form the organic phase. The aqueous phase consisted of HNO_3 solution with specific radionuclide concentrations: Pu(IV), 5 mg L; Np(V), 0.5 g L; U(VI), 1 g L^{-1} and Am(III), trace amount. All solvent extraction experiments were conducted at 298 K with 0.05 M of extractant in organic solvent, except when studying the effects of temperature and ligand concentration, respectively. Prior to the extraction experiments, each organic phase underwent two pre-equilibrium steps with equal volumes of HNO_3 solution. Subsequently, the organic and aqueous phases were mixed in a test tube in equal volumes and extracted for 15 min at 2000 rpm, followed by centrifugation for 5 min at 2500 rpm. From each phase, samples (100 μL) were equally divided into organic and aqueous phases and analyzed by liquid scintillation spectrometry. All samples were tested twice. The distribution ratio of metal ions (D_M) was defined as the ratio of the metal contents of the organic and aqueous phases (*i.e.*, $D_M = [M]_{org}/[M]_{aq}$), and the separation factor (SF) was defined as the ratio of their distribution ratios (*i.e.*, $SF_{A/B} = D_A/D_B$).

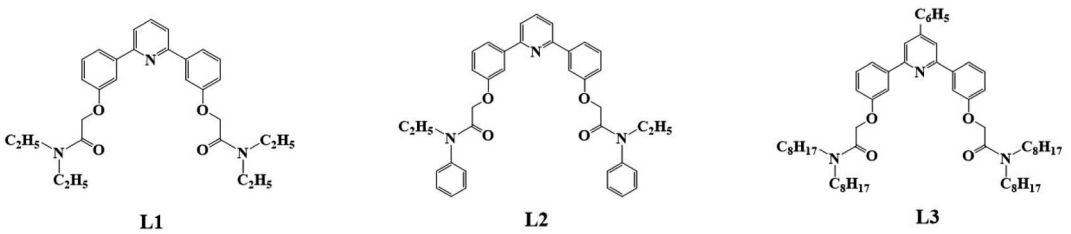

Fig. 2 Structure of phenylpyridine diamide extractants L1–L3.

UV-vis spectrophotometric titration

UV-vis spectrophotometric titration was performed at room temperature (298 K). The extractant concentration was set at 2.0×10^{-5} M, and the metal ion concentration was 2.0×10^{-3} M. A quartz colorimetric dish with an optical path of 1.0 cm was used for titration. The initial ligand volume was 2.5 mL. The metal ion solution was added to the quartz cuvette in 20 μL intervals until no obvious changes were observed in the UV spectrum. After each addition, the solution was mixed at 2000 rpm, allowed to stand for 15 min, and then analyzed 2 min later by UV spectrometry. The spectral data were fitted and analyzed using hyperSpec software.[41]

Stripping

After extraction, the Pu-containing organic phase was collected and subjected to stripping (reverse extraction) experiments. Five back-extracting agents were used: 0.2 M dimethylacetamide (DMHAN)–0.1 M dimethylacetamide (MMH), 0.2 M HNO_3, 0.1 M ethylene diamine tetraacetic acid (EDTA)–0.5 M HNO_3, 0.2 M $H_2C_2O_4$–0.5 M HNO_3, and 0.2 M acetohydroxamic acid (AHA)–0.5 M HNO_3. Equal volumes of organic and aqueous phases were mixed and agitated for 15 min. After centrifugation, samples (100 μL) from each phase were analyzed by liquid scintillation. All extracted samples were measured twice.

Results and discussion

Solvent extraction experiments

The extraction kinetics were explored by varying the contact time (Fig. 3a). For all extractants, the equilibrium time for Pu(IV) extraction was approximately 1 min, signifying rapid extraction kinetics. This was attributed to the positioning of the two coordinating amide oxygen atoms in the pyridine ring plane, which led to efficient coordination without C=O bond twisting and thus with reduced energy consumption. All subsequent experiments used a contact time of 15 min to ensure the extraction equilibrium was reached.

Fig. 3b presents the Pu(IV) distribution ratios (D_{Pu}) of the ligand (L)/1-(trifluoromethyl)-3-nitrobenzene systems as a function of the HNO_3 concentration. As the HNO_3 concentration increased from 0.2 to 6 M, D_{Pu} first increased until reaching a maximum at approximately 4 M, after which it slightly decreased. No third phase was observed to form during the extraction process. The ligands with longer carbon chains (**L2** (PEPA) and **L3** (PPOA)) had higher D_{Pu} values than those with shorter carbon chains (**L1** (PPEA)). This was attributed to the enhanced solubility of long-chain ligands in 1-(trifluoromethyl)-3-nitrobenzene, which improves the distribution of Pu(IV). At 6 M HNO_3, D_{Pu} was noticeably lower than that at 4 M. This was ascribed to the increased content of hydrogen ions, which compete with free Pu(IV) ions.

Fig. 3c shows the effect of the NO_3^- content on D_{Pu}. The slopes of the fitted curves in the $\log D$ *vs.* $\log[NO_3^-]$ plots for **L1**, **L2**, and **L3** were 3.95, 4.12, and 3.93 respectively (inset of Fig. 3c), indicating that four NO_3^- ions participated in the complexation reactions with each ligand. Thus, increasing the NO_3^- content improved D_{Pu} and promoted the complexation reaction by a salting-out mechanism. Notably, this indicates that complexation occurred by a neutral extraction mechanism.

To determine the stoichiometry of the extracted complexes, slope analysis was conducted on the extraction equilibrium data (Fig. 3d). The extraction equilibrium reaction and apparent equilibrium constant K_{ex} are given in eqn (1) and (2), respectively. The distribution ratio is given by eqn (3) and it can be rearranged to eqn (4). The slopes of the $\log D$ *vs.* $\log[L]$ plots for **L1**, **L2**, and **L3** were 1.15, 1.19, and 1.20, respectively (inset of Fig. 3d). Sivaramakrishna *et al.*[40] obtained similar slope values (1.20 and 1.24) during their study on the extraction of Pu(IV) using different concentrations of TAPDA in nitrobenzene. Taking into account the error range, the dominant stoichiometric ratio of Pu(IV) to L in the extracted complexes is 1 : 1, characterized by the formation of $Pu(NO_3)_4L$ complexes. Two factors contribute to this 1 : 1 complex formation. First, the ligands have high solubility in 1-(trifluoromethyl)-3-nitrobenzene. Second, each Pu(IV) ion can only form a complex with one ligand, as the large steric hindrance of the alkyl side chains prevents the Pu(IV) ions from coordinating with additional ligands.

$$Pu_{aq}^{4+} + 4NO_3^- + nL_{org} \rightleftharpoons Pu(NO_3)_4 \cdot nL_{org} \quad (1)$$

$$K_{ex} = \frac{[Pu(NO_3)_4 \cdot nL]_{org}}{[Pu^{4+}]_{aq}[NO_3^-]_{aq}^{4+}[L]_{org}^{n}} \quad (2)$$

$$D = \frac{[Pu(NO_3)_4 \cdot nL]_{org}}{[Pu^{4+}]_{aq}} \quad (3)$$

$$\log D = \log K_{ex} + 4\log[NO_3^-]_{aq} + n\log[L]_{org} \quad (4)$$

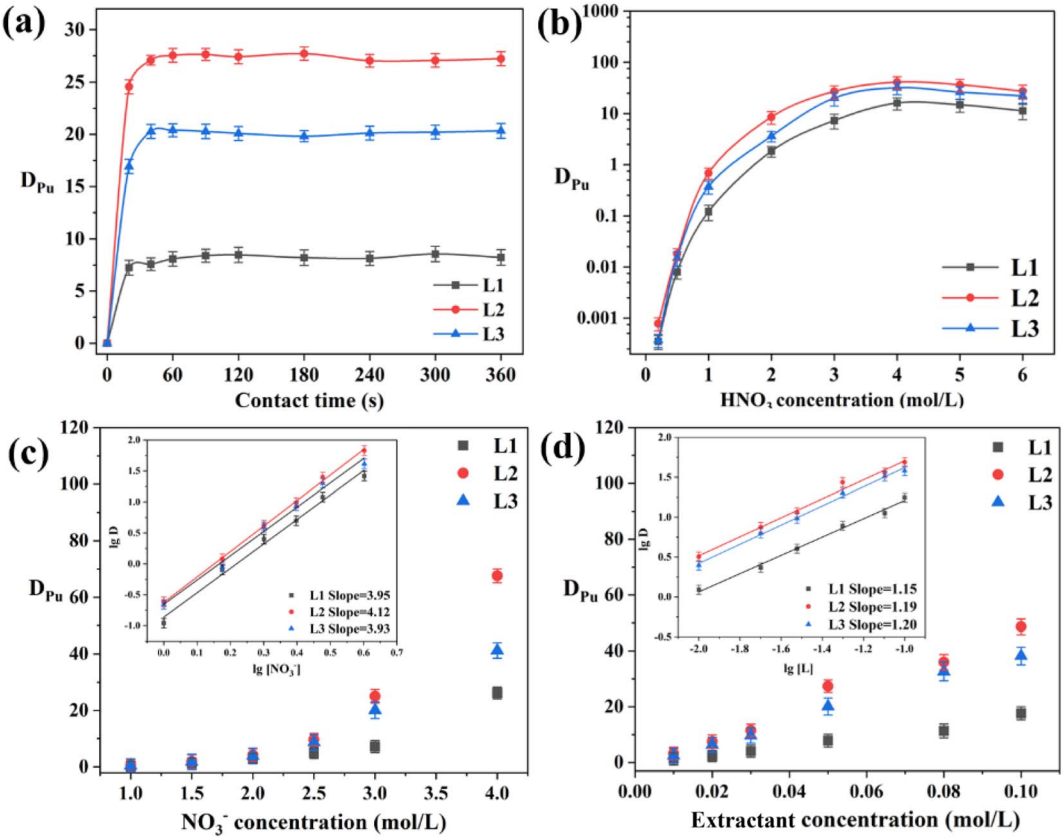

Fig. 3 (a) Kinetics of Pu(IV) extraction by phenylpyridine diamide ligands **L1**, **L2**, and **L3**. (b) Pu(IV) distribution ratios (D_{Pu}) obtained for extractants at different HNO_3 concentrations. (c) Influence of NO_3^- concentration on extraction performance. (d) Effect of extractant concentration on extraction performances of **L1**, **L2**, and **L3**.

where n is the number of ligands in the complexation reaction, [X] is the concentration of X, and D is the distribution factor.

To explore the influence of temperature on the extraction performance, experiments were carried out at temperatures of 298–338 K using 1-(trifluoromethyl)-3-nitrobenzene as the diluent. Utilizing the Van't Hoff equation (eqn (5)), the enthalpy change (ΔH) was derived from the slope of the log K_{ex} *vs.* $1/T$ plots, where T is temperature (Fig. 4). The ΔH values for extractants **L1**, **L2**, and **L3** were −5.97, −11.24, and −9.15 kJ mol^{-1}, respectively. This confirms the exothermic nature of the complexation reaction. The entropy change ΔS and Gibbs free energy ΔG of the complexation reaction were calculated using eqn (6), and the thermodynamic data are listed in Table 1. The ΔS values for the reactions with all three extractants were negative because the complexation between metal ions and NO_3^- reduces the disorder of the system. In addition, the ΔG values were negative for all three reactants, signifying that the Pu(IV) complexation reaction occurs spontaneously at room temperature. Notably, **L2** (PEPA) had the most negative ΔG value, indicating that this ligand is the most efficient for extracting Pu(IV).

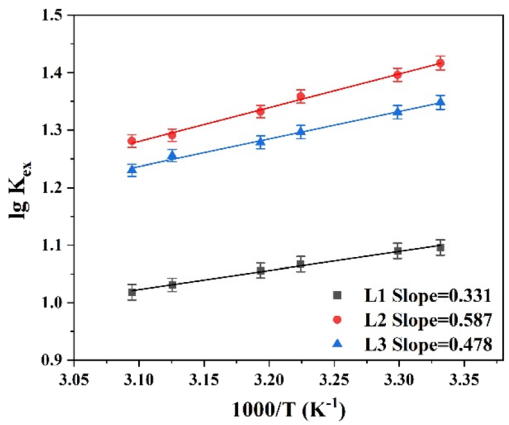

Fig. 4 Effect of temperature on Pu(IV) extraction performance of phenylpyridine diamide ligands **L1**, **L2**, and **L3**.

Table 1 Thermodynamic parameters of extraction reactions with different phenylpyridine diamide ligands

Ligand	ΔH (kJ mol^{-1})	ΔS (kJ mol^{-1})	ΔG (kJ mol^{-1})
L1	−5.97	−0.09	−5.94
L2	−11.24	−10.33	−8.16
L3	−9.15	−4.67	−7.75

$$\log K_{ex} = -\frac{\Delta H}{2.303R} \times \frac{1}{T} + \frac{\Delta S}{2.303R} \quad (5)$$

$$\Delta G = \Delta H - T\Delta S \quad (6)$$

UV-Vis spectrophotometric titration analysis

To further study the Pu(IV) extraction mechanism of the three diamide extractants and ascertain the species composition and stability constant ($\log \beta$), UV spectrophotometric titration was performed. As shown in Fig. 5, the initial UV absorption peak of each extractant is observed at approximately 325 nm (the black curve), corresponding to the C=O bond of the ligand. With increasing metal ion concentration, the peak at 325 nm gradually decreased in intensity, while a new peak of the metal-ligand bond appeared at 298 nm and increased in intensity as the titration process continued. The peak type and shift were consistent for all three extractants, indicating that the carbon chain substituents did not affect the structure of the complex. Table 2 lists the $\log \beta$ values of the complexes, which further confirms that the three extractants typically generated 1 : 1 complexes with Pu(IV). **L2** (PEPA) had a larger $\log \beta$ value than the other extractants, indicating that it formed the most stable complex with Pu(IV). This observation aligns with the results in solvent extraction experiments.

Selectivity

The selectivity of the three diamide extractants for Pu(IV) was assessed by investigating their extraction behavior for different actinide ions (Pu(IV), U(VI), Np(V), and Am(III)) and certain fission products in HNO_3 solution using 1-(trifluoromethyl)-3-nitrobenzene as the diluent. Considering the competition for binding between hydrogen and metal ions at high acidities, the HNO_3 concentration was fixed at 3 M. The distribution ratios and separation factors of different actinides, lanthanides, and fission elements are displayed in Table 3. The results showed that the three diamide extractants exhibited high selectivity for Pu(IV) in 3 M HNO_3. As shown in Fig. 6, D_{Pu} reached 27.1 using **L2** (PEPA), while the D_U, D_{Np}, and D_{Am} values were 1.11, 0.3, and 0.02, respectively. All the ligands extracted Pu(IV) more effectively than other metals, while Am(III) and the fission product ions were hardly extracted (distribution ratios of <0.1).

Table 2 Stability constants $\log \beta$ of complexes with different phenylpyridine diamide ligands

Ligand	Reaction	$\log \beta$
L1	$Pu + 4NO_3 + nL \rightleftharpoons Pu(NO)_4 \cdot nL$	4.09 ± 0.03
L2		6.29 ± 0.02
L3		5.36 ± 0.05

Phenanthroline ligands (*e.g.*, Et-Tol-DAPhen) exhibit similarly high extraction abilities for Pu(IV); however, they also extract Am(III) and U(VI). By comparison, the diamide ligands in this study have high separation factors for Pu(IV) over Am(III) and U(VI). The separation factors for Pu(IV) over other actinides and fission elements are also higher than those of tripyridine diamide ligands (*e.g.*, te-tpyda and to-tpyda).[38,39] These results demonstrate that diamide ligands **L1–L3** can all effectively extract Pu(IV) from the aqueous phase while leaving other actinides and fission metal ions predominantly in solution. Thus, the extractants have good application prospects for the selective separation of Pu(IV).

Stripping experiment

To further explore the practical application of the extractants, stripping extraction tests were conducted. Based on the solvent extraction results, the D_{Pu} values were lower at lower acidities and NO_3^- concentrations. Consequently, the stripping extraction of Pu(IV) is feasible at low HNO_3 concentrations. We evaluated the Pu(IV) stripping ability of the three diamide extractants using five stripping agents. The results are displayed in Tables 4, S3 and S4.† After three stages of stripping, nearly complete Pu(IV) stripping was achieved, demonstrating the excellent stripping performance of the extractants. Notably, nearly 100% stripping efficiency was achieved when using 0.2 M HNO_3 as the stripping agent. These outcomes highlight the viability of reusing the same extractants in multiple Pu(IV) separation cycles.

The reusability of the three diamide extractants was further investigated over ten extraction – back extraction cycles. The cyclic Pu(IV) and U(VI) extraction abilities of ligands **L1–L3** are shown in Fig. 7 and S3.† The D_{Pu} and $SF_{Pu/U}$ values remained nearly constant over the ten cycles, demonstrating the excellent reusability of the three diamide extractants.

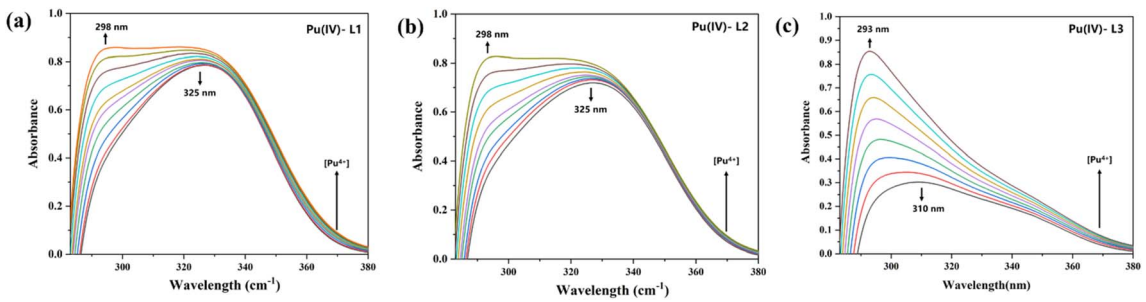

Fig. 5 Spectrophotometric titration of ligands (a) **L1**, (b) **L2**, and (c) **L3** ([L] = 2.0×10^{-5} M) with $Pu(NO_3)_4$ ([M] = 2×10^{-3} M) at $T = 298$ K.

Table 3 Distribution ratios D and separation factors SF of some actinides, lanthanides, and fission elements by phenylpyridine diamide ligands **L1**, **L2**, and **L3** in 3.0 M HNO_3 solution

	L1		L2		L3	
	D	SF	D	SF	D	SF
Pu(IV)	7.28	—	27.12	—	20.08	—
U(VI)	0.95	7.66	1.11	24.39	1.12	17.88
Pu(III)	0.20	37.33	1.95	13.90	1.93	10.41
Np(V)	0.15	49.52	0.30	91.93	0.27	75.21
Np(VI)	0.01	606.67	0.03	968.57	0.02	836.67
Am(III)	0.01	808.89	0.02	1695.00	0.01	1825.45
Zr(IV)	0.63	11.48	0.61	44.25	0.62	32.54
Cr(III)	0.43	16.88	0.41	66.18	0.41	48.50
Mo(III)	0.18	41.47	0.05	494.44	0.08	260.88
Ce(III)	0.12	60.97	0.04	755.22	0.05	389.15
Ru(III)	0.11	63.63	0.04	674.29	0.05	370.07
Pr(III)	0.07	97.72	0.07	405.62	0.07	293.65
Sm(III)	0.07	111.42	0.07	379.67	0.07	286.00
Eu(III)	0.06	122.72	0.05	529.48	0.04	456.47
Nd(III)	0.06	122.72	0.06	468.96	0.06	345.43
Sr(II)	0.05	158.16	0.05	508.15	0.05	386.97

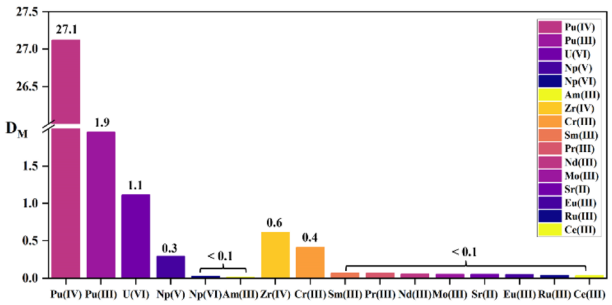

Fig. 6 Extraction properties of some actinides, lanthanides, and fission elements by **L2** (PEPA) in 3.0 M HNO_3 solution.

Radiation stability

Radiation-induced degradation can affect the structure and extraction performance of extractants. Therefore, radiolytic stability is crucial for their reusability. The radiation stability can be evaluated by characterizing the structure of the extractant or the distribution ratio of metal ions after irradiation. In this study, the three extractants in 1-(trifluoromethyl)-3-nitrobenzene were exposed to varying doses of γ radiation (0.1, 1, 10, and 100 kGy) from a ^{60}Co γ irradiator while monitoring the D_{Pu} values. As shown in Fig. 8, after receiving a dose of 100 kGy, the D_{Pu} and $SF_{Pu/U}$ values of **L2** decreased by only 4.96% and 1.4%, respectively. This suggests that the Pu(IV) and U(VI) extraction efficiencies remained consistent after

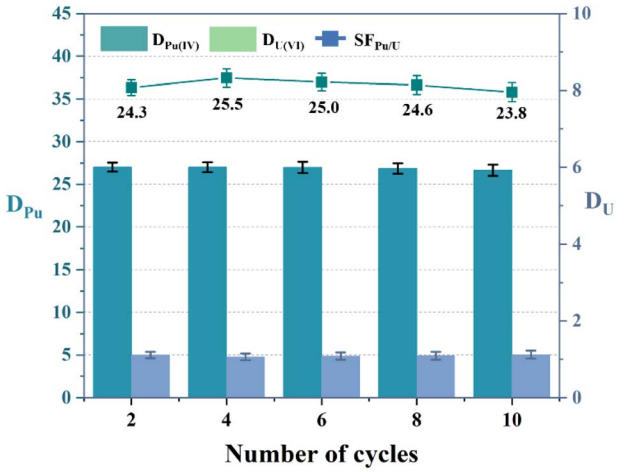

Fig. 7 Reusability of extractant **L1** (PPEA). Organic phase: 0.05 M **L1** in 1-(trifluoromethyl)-3-nitrobenzene; aqueous phase: 3 M HNO_3, 5 mg L^{-1} Pu(IV), and 1 g L^{-1} U(VI).

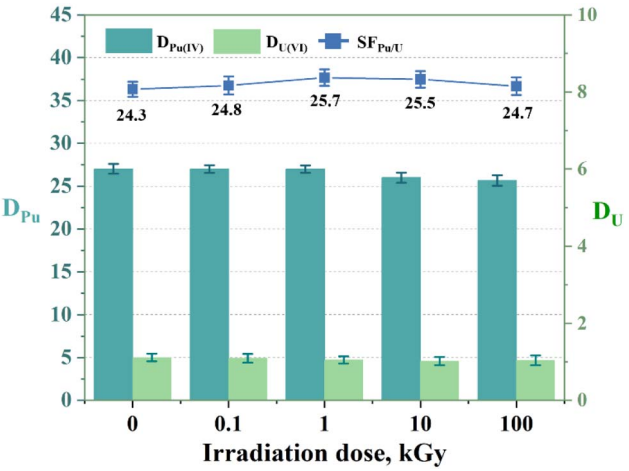

Fig. 8 Extraction of Pu(IV) and U(VI) using **L2** (PEPA) exposed to γ irradiation for different durations. Organic phase: 0.05 M **L2** in 1-(trifluoromethyl)-3-nitrobenzene; aqueous phase: 3 M HNO_3, 5 mg L^{-1} Pu(IV), and 1 g L^{-1} U(VI).

Table 4 Pu(IV) stripping efficiency of **L2** (PEPA) in 1-(trifluoromethyl)-3-nitrobenzene using five stripping agents

	Stripping agent				
Stage	0.2 M DMHAN–0.1 M MMH	0.2 M HNO_3	0.1 M EDTA–0.5 M HNO_3	0.2 M $H_2C_2O_4$–0.5 M HNO_3	0.2 M AHA–0.5 M HNO_3
1	87.5%	83.6%	82.5%	76.9%	84.9%
2	71.2%	70.5%	65.3%	68.9%	73.6%
3	82.5%	71.5%	82.5%	71.4%	87.7%
Total after 3 stages	99.4%	98.7%	98.9%	97.9%	99.5%

irradiation. The results for the other extractants are displayed in Fig. S4.† Overall, all three extractants exhibited good radiation resistance. This may be because extractants containing aromatic groups, such as those in this study, typically have better radiolytic stability than those containing aliphatic groups.[40] This resistance further demonstrates the potential of these ligands for sustained and long-term utilization.

Conclusions

In this study, we synthesized and evaluated three diamide extractants bearing phenylpyridine rings with different functional groups for the separation of Pu(IV) in a complex system in HNO_3 solution using 1-(trifluoromethyl)-3-nitrobenzene as a diluent. The ligands exhibited high selectivity for Pu(IV) over other metals such as U(VI), Np(V), Am(III), and various fission elements. Notably, the ligands with longer carbon chains (**L2** (PEPA) and **L3** (PPOA)) extracted Pu(IV) more effectively than those with shorter carbon chains (**L1** (PPEA)) because the long carbon chains enhanced the solubility of the ligands in the diluent and thus improved D_{Pu}. The slope analysis and UV-vis spectrophotometric titration results revealed the formation of 1 : 1 complexes between the extractants and Pu(IV). This was attributed to the steric hindrance of the long alkyl chains, which restricted coordination between Pu(IV) and additional ligand molecules. Thermodynamic evaluations confirmed that the extraction reaction was exothermic and occurred spontaneously at room temperature. **L2** had the most negative Gibbs free energy of the three ligands, which aligns with its high extraction performance for Pu(IV). All three diamide extractants exhibited good stripping ability and reusability, and their radiolytic stability was appreciable up to an absorbed dose of 100 kGy. This highlights the excellent application prospects of phenylpyridine diamide ligands in the selective extraction of Pu(IV). Furthermore, the results contribute to the study of actinide coordination with diamide ligands and improve our understanding of actinide chemistry during coordination, offering new ideas for the design and synthesis of novel extractants.

Conflicts of interest

There are no conflicts to declare.

Acknowledgements

This work was supported by China Institute of Atomic Energy Head foundation (YZ232605000803). We are grateful to their financial help and constant encouragement.

References

1 R. Rama, A. Rout, K. A. Venkatesan and M. P. Antony, *Sep. Purif. Technol.*, 2017, **172**, 7.
2 P. Baron, S. M. Cornet, E. D. Collins, G. DeAngelis, G. Del Cul, Yu. Fedorov, J. P. Glatz, V. Ignatiev, T. Inoue, A. Khaperskaya, I. T. Kim, M. Kormilitsyn, T. Koyama, J. D. Law, H. S. Lee, K. Minato, Y. Morita, J. Uhlíř, D. Warin and R. J. Taylor, *Prog. Nucl. Energy*, 2019, **117**, 103091.
3 L. Rodríguez-Penalonga and B. Y. Moratilla Soria, *Energies*, 2017, **10**, 1235.
4 I. Kumari, B. V. R. Kumar and A. Khanna, *Nucl. Eng. Des.*, 2020, **358**, 110410.
5 E. A. Mowafy and H. F. Aly, *Solvent Extr. Ion Exch.*, 2001, **19**, 629.
6 K. Bell, C. Carpentier, M. Carrott, A. Geist, C. Gregson, X. Hérès, D. Magnusson, R. Malmbeck, F. McLachlan, G. Modolo, U. Müllich, M. Sypula, R. Taylor and A. Wilden, *Procedia Chem.*, 2012, **7**, 392.
7 Z. Zhu, Y. Pranolo and C. Y. Cheng, *Miner. Eng.*, 2015, **77**, 185.
8 M. Salvatores, *Nucl. Eng. Des.*, 2005, **235**, 805.
9 M. Salvatores and G. Palmiotti, *Prog. Part. Nucl. Phys.*, 2011, **66**, 144.
10 B. Mahanty, P. K. Verma, P. K. Mohapatra, A. Leoncini, J. Huskens and W. Verboom, *Sep. Purif. Technol.*, 2020, **238**, 116418.
11 A. Karak, B. Mahanty, P. K. Mohapatra, Sk. Musharaf Ali, R. J. M. Egberink, D. B. Sathe, R. B. Bhatt, T. P. Valsala, J. Huskens and W. Verboom, *New J. Chem.*, 2022, **46**, 21221.
12 S. Usuda, K. Yamanishi, H. Mimura, Y. Sasaki, A. Kirishima, N. Sato and Y. Niibori, *J. Radioanal. Nucl. Chem.*, 2015, **303**, 1351.
13 V. N. Bliznyuk, K. Kołacińska, A. A. Pud, N. A. Ogurtsov, Y. V. Noskov, B. A. Powell and T. A. DeVol, *RSC Adv.*, 2019, **9**, 30052.
14 V. K. Rao, I. C. Pius, M. Subbarao, A. Chinnusamy and P. R. Natarajan, *J. Radioanal. Nucl. Chem.*, 1986, **100**, 129.
15 M. Sivaramakrishna, D. R. Raut, S. Nayak, S. K. Nayak and P. K. Mohapatra, *Sep. Purif. Technol.*, 2017, **181**, 69.
16 A. Rout, K. Chatterjee, K. A. Venkatesan, K. K. Sahu, M. P. Antony and P. R. Vasudeva Rao, *Sep. Purif. Technol.*, 2016, **159**, 43.
17 A. E. Visser and R. D. Rogers, *J. Solid State Chem.*, 2003, **171**, 109.
18 S. A. Ansari, P. K. Mohapatra, V. Mazan and I. Billard, *RSC Adv.*, 2015, **5**, 35821.
19 Y. Sasaki, Y. Morita, Y. Kitatsuji and T. Kimura, *N,N,N′,N′*-tetraoctyl-3,6-dioxaoctanediamide (DOODA), *Solvent Extr. Ion Exch.*, 2010, **28**, 335.
20 C. Berger, C. Marie, D. Guillaumont, C. Tamain, T. Dumas, T. Dirks, N. Boubals, E. Acher, M. Laszczyk and L. Berthon, *Inorg. Chem.*, 2020, **59**, 1823.
21 R. B. Gujar, S. A. Ansari, M. S. Murali, P. K. Mohapatra and V. K. Manchanda, *J. Radioanal. Nucl. Chem.*, 2010, **284**, 377.
22 R. Ruhela, S. Panja, B. S. Tomar, M. A. Mahajan, R. M. Sawant, S. C. Tripathi, A. K. Singh, P. M. Gandhi, R. C. Hubli and A. K. Suri, *Tetrahedron Lett.*, 2012, **53**, 5434.
23 S. A. Ansari, A. Bhattacharyya, P. K. Mohapatra, R. J. M. Egberink, J. Huskens and W. Verboom, *RSC Adv.*, 2019, **9**, 31928.
24 B. Ya. Zilberman, N. D. Goletskiy, E. A. Puzikov, A. A. Naumov, E. A. Kamaeva, A. S. Kudinov,

Yu. Yu. Petrov, P. V. Aksyutin, V. N. Alekseenko and E. S. Skurydina, *Solvent Extr. Ion Exch.*, 2019, **37**, 435.
25 X. Liu, J. Liang and J. Xu, *Solvent Extr. Ion Exch.*, 2004, **22**, 163.
26 C. Xu, C. Wang, J. Wang and J. Chen, *Sep. Sci. Technol.*, 2013, **48**, 183.
27 M. Wei, X. Liu and J. Chen, *J. Radioanal. Nucl. Chem.*, 2012, **291**, 717.
28 T. Sun, Y. Zhang, Q. Wu, J. Chen, L. Xia and C. Xu, *Solvent Extr. Ion Exch.*, 2017, **35**, 408.
29 G. J. Lumetta, A. V. Gelis, J. C. Braley, J. C. Carter, J. W. Pittman, M. G. Warner and G. F. Vandegrift, *Solvent Extr. Ion Exch.*, 2013, **31**, 223.
30 Y. Morita, J. P. Glatz, M. Kubota, L. Koch, G. Pagliosa, K. Roemer and A. Nicholl, *Solvent Extr. Ion Exch.*, 1996, **14**, 385.
31 K. J. Parikh, P. N. Pathak, S. K. Misra, S. C. Tripathi, A. Dakshinamoorthy and V. K. Manchanda, *Solvent Extr. Ion Exch.*, 2009, **27**, 244.
32 V. Vanel, C. Marie, P. Kaufholz, M. Montuir, N. Boubals, A. Wilden, G. Modolo, A. Geist and C. Sorel, *Procedia Chem.*, 2016, **21**, 223.
33 S. D. Reilly, A. J. Gaunt, B. L. Scott, G. Modolo, M. Iqbal, W. Verboom and M. J. Sarsfield, *Chem. Commun.*, 2012, **48**, 9732.
34 S. Sharma, S. Panja, A. Bhattacharyya, P. S. Dhami, P. M. Gandhi and S. K. Ghosh, *Dalton Trans.*, 2016, **45**, 7737.
35 P. N. Pathak, *J. Radioanal. Nucl. Chem.*, 2014, **300**, 7.
36 Y. Sasaki, Y. Sugo, S. Suzuki and S. Tachimori, *Solvent Extr. Ion Exch.*, 2001, **19**, 91.
37 X. Zhang, Q. Wu, J. Lan, L. Yuan, C. Xu, Z. Chai and W. Shi, *Sep. Purif. Technol.*, 2019, **223**, 274.
38 X. Zhang, L. Yuan, Z. Chai and W. Shi, *Sep. Purif. Technol.*, 2016, **168**, 232.
39 C. Marie, M. Miguirditchian, D. Guillaneux, J. Bisson, M. Pipelier and D. Dubreuil, *Solvent Extr. Ion Exch.*, 2011, **29**, 292.
40 M. Sivaramakrishna, D. R. Raut, S. K. Nayak, S. K. Nayak and P. K. Mohapatra, *Radiochim. Acta*, 2017, **105**, 303.
41 L. Alderighi, P. Gans, A. Ienco, D. Peters, A. Sabatini and A. Vacca, *Coord. Chem. Rev.*, 1999, **184**, 311.